remote sensing

MDPI

Article

Evolution of Coastal Cliffs Characterized by Lateral Spreading in the Maltese Archipelago

Luciano Galone [1,*], Federico Feliziani [2], Emanuele Colica [1], Enrique Fucks [3,4], Jesús Galindo-Zaldívar [5,6], Ritienne Gauci [7], Christopher Gauci [8], Guglielmo Grechi [2], Salvatore Martino [2], Lluís Rivero [9,10] and Sebastiano D'Amico [1]

1 Department of Geosciences, University of Malta, MSD 2080 Msida, Malta; sebastiano.damico@um.edu.mt (S.D.)
2 Department of Earth Sciences, Sapienza University of Rome, 00185 Rome, Italy
3 Facultad de Ciencias Naturales y Museo, National University of La Plata, La Plata 1900, Argentina
4 Centro de Estudios Integrales de la Dinámica Exógena, National University of La Plata (CEIDE-CIC-UNLP), La Plata 1900, Argentina
5 Department of Geodynamics, University of Granada, 18071 Granada, Spain
6 Andalusian Earth Sciences Institute, Spanish National Research Council (CSIC), University of Granada, 18100 Armilla, Spain
7 Department of Geography, Faculty of Arts, University of Malta, MSD 2080 Msida, Malta
8 Research and Planning Unit, Public Works Department, Ministry for Public Works and Planning, FRN 1700 Floriana, Malta
9 Mineralogy, Petrology and Applied Geology, Universitat de Barcelona, 08028 Barcelona, Spain
10 Water Research Institute, Universitat de Barcelona, 08001 Barcelona, Spain
* Correspondence: luciano.galone@um.edu.mt

Abstract: The Maltese archipelago is renowned for its spectacular coasts, characterized by vertical cliffs and scree slopes. In the western sector of Malta and the eastern region of Gozo, a marly clay formation with ductile properties underlying a stiff limestone unit has led to relevant lateral spreading. Utilizing drone aerial photogrammetry, digital elevation models, and satellite imagery, we analyzed the ongoing geomorphological processes across five promontories, selected as case studies. Our analysis reveals a complex interaction between geological structures, Quaternary sea level fluctuations, and lateral spreading processes. Photogrammetric models show that once detached, blocks from the plateaus tend to topple and fall or experience subsidence and backtilting. At Rdum il-Qammieħ, fractures up to 250 m long and openings of up to 2 m were observed, while at Sopu, detached blocks exhibit subsidence of up to 50% and rotations nearing 60°. In all the studied promontories, rotational slides predominantly occur at the frontal sectors, while toppling mechanisms are more common along scarp-edged plateaus. The thickness ratio between the stiff and the ductile formation, ranging from 0.13 to 1.12, along with slope gradients between 10° and 41°, further influence the stability of these coastal features. We discuss the structural and sea level influences on Maltese coastal cliff development over the last 125 ky. We propose a conceptual model outlining the evolution of the Malta Graben promontories through a three-stage evolutionary model: proto-promontories, cliff demolition, and isolation. This model emphasizes the significant role of predisposing, preparatory, and triggering factors in the geomorphological evolution of the Maltese coastline. Our findings provide essential insights into the landscape changes in the Maltese archipelago and represent a useful tool for coastal management and hazard mitigation strategies.

Keywords: coastal geomorphology; rotational slide; toppling; sea level oscillations; lateral spreading

Citation: Galone, L.; Feliziani, F.; Colica, E.; Fucks, E.; Galindo-Zaldívar, J.; Gauci, R.; Gauci, C.; Grechi, G.; Martino, S.; Rivero, L.; et al. Evolution of Coastal Cliffs Characterized by Lateral Spreading in the Maltese Archipelago. *Remote Sens.* **2024**, *16*, 3072. https://doi.org/10.3390/rs16163072

Academic Editor: Deepak R. Mishra

Received: 22 July 2024
Revised: 15 August 2024
Accepted: 17 August 2024
Published: 21 August 2024

1. Introduction

Rocky coasts, with characteristic landforms such as plunging cliffs and expansive shore platforms [1], experienced modifications during the Quaternary due to sea level oscillations, which contributed to the erosion and reconfiguration of pre-existing landscapes.

However, other factors such as underlying lithology, geological structures, and climate also play an important role. In particular, promontories (also referred to as "headlands") stand out for their prominence and uniqueness in the coastal scenery. Unlike linear coastlines, promontories extend into the sea, creating visually striking extensions of land that penetrate the waters. This distinctive configuration enhances their aesthetic appeal and signifies a diversity of processes shaping the coastline at various scales, revealing unique geological and geomorphological signatures that offer valuable insights into coastal evolution.

The retreat processes that involve the plateaus at the promontory tops are influenced by a series of interconnected factors, the understanding of which is crucial for addressing the geological dynamics of these landscapes. These factors can generally be grouped into three categories: predisposing, preparatory, and triggering factors [2]. Predisposing factors do not change with time; rather, they determine the overall structure of the slope that stimulates the beginning of instabilities to different extents. This is the case of geo-structural conditions, as well as the topographical features of a slope. Preparatory factors are widely understood to be the sources of medium- to long-term changes in resistance or disturbing forces, such as meteo-climatic conditions and their medium-long-term variations. Lastly, triggering factors are the most direct causes of failure and are frequently those that are associated with short- to medium-term changes.

Within slope processes, lateral spreading deformations (sensu [3,4]) frequently occur where resistant and brittle rocks overlie softer and more deformable materials like clays or marl. This rheological contrast induces fracturing processes that cause the detachment of blocks from resistant lithology, which then separate laterally and evolve toward more specific landslide mechanisms. These processes have been extensively studied in various Mediterranean countries (e.g., [5–9]).

Malta (Figure 1) is an insular Mediterranean state renowned for its distinctive coastal geomorphological features (e.g., [10–12]). In particular, the presence of rigid limestone rocks forming plateaus over ductile clayey rocks promotes the initialization of several lateral spreading phenomena especially in the western sector of the island of Malta and the eastern region of Gozo. These landforms initiate the development of gravity-induced fractures [13] along plateau edges, resulting in block separation and evolving into rotational slides, falls, and blocks overturning. The relatively compact size and the spectacular processes associated with coastal cliffs and marine promontories in the Maltese archipelago have spurred a significant number of studies in recent decades, e.g., [6,14–22]. These studies employ geomatic techniques, geophysical methods, satellite measurements, and seismic monitoring to assess cliff erosion, map fractures, and monitor the dynamic characteristics of unstable coastal environments, thereby providing crucial data for coastal management and future landslide risk assessments. In most cases, these studies focus on the dominant processes and the evolutionary scenarios responsible for the development of promontories as contemporary landforms. Understanding these processes is essential to comprehensively investigate the geological dynamics of these unique coastal landscapes from a risk management perspective given that their susceptibility to coastal retreat threatens urban infrastructure as well as cultural heritage. This contribution aims to study the evolution of the Maltese coastal cliffs characterized by the lateral spreading phenomena. To achieve this, we focus on the most prominent promontories of the archipelago, where these processes are most pronounced.

By elucidating the key geomorphological processes and their interactions over time, we seek to provide insights into the formation and development of these distinctive coastal features, contributing to broader understandings of coastal evolution and facilitating more effective coastal management strategies.

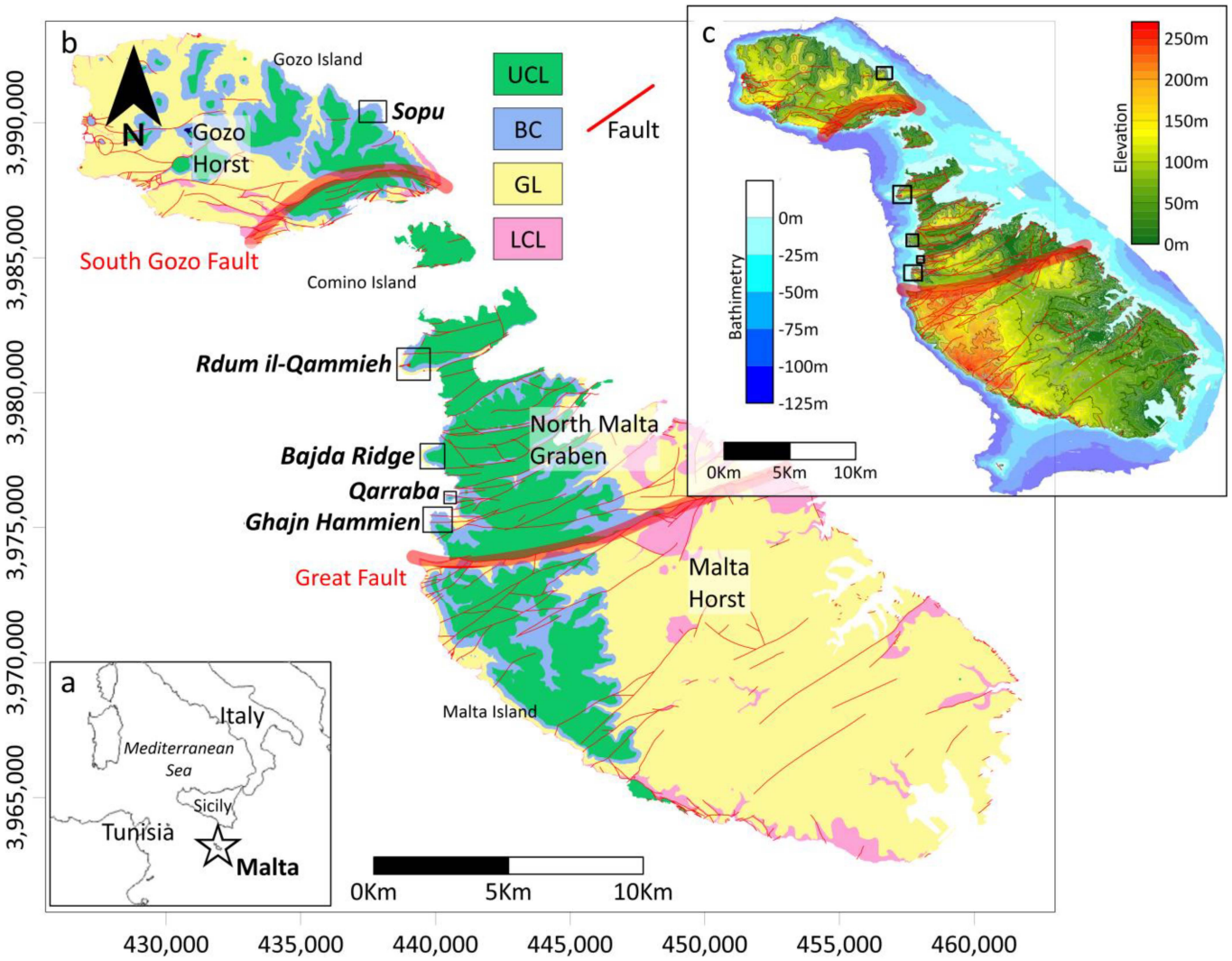

Figure 1. The Maltese archipelago. (**a**) Location of Malta (indicated by a star) in the Mediterranean. (**b**) Geological map of the Maltese archipelago, with the locations of the studied promontories marked by black rectangles. Main structural features are depicted. LCL: Lower Coraline Limestone Fm.; GL: Globigerina Fm.; BC: Blue Clay Formation; and UCL: Upper Coraline Formation. (**c**) Topographic and bathymetric map of the Maltese archipelago, with the studied promontories indicated by rectangles.

2. Geological and Geomorphological Settings

The Maltese archipelago (Figure 1), located approximately 100 km south of the coast of Sicily in the central Mediterranean, is an extensive extensional crustal domain that evolved from the late Miocene onward, undergoing significant crustal stretching during the Plio-Quaternary [23–25].

The islands are mostly composed of Oligocene–Miocene shallow-water bioclastic and coralline carbonates and deep-water clays arranged in a sub-horizontal to gently dipping sequence [26]. The main formations are the Lower Coralline Limestone Fm. (LCL), a hard and compact limestone (late Oligocene); the Globigerina Limestone Fm. (GL), a soft fine-grained limestone (early Miocene); Blue Clay Fm. (BC), a soft pelagic marl and limey clay (middle-late Miocene); and Upper Coralline Limestone Fm. (UCL), a coarse-grained limestone (late Miocene).

Due to their proximity to the sea and small drainage basins, sediment deposits from short rivers have been largely eroded, especially during periods of lowered sea levels in cold climatic phases [27]. Preserved sediment remnants are primarily found in caves or as relics of conglomerates with reddish matrices attributed to the Middle–Late Pleistocene

(the so-called red beds; Refs. [27–30]). The area has remained relatively tectonically stable for the last 125 Ky [31,32].

The archipelago is structurally characterized by two major fault systems that control the principal tectonic domains: a WSW-ENE and a WNW-ESE, both trending normal faults that shape its geological and geomorphological features. The Great Fault (WSW-ENE), crossing Malta approximately through its central sector, marks the NW boundary of the Malta Horst (Figure 1). Northwards, the South Gozo Fault defines the SE boundary of the Gozo Horst. Between these domains lies the Malta Graben, encompassing northern Malta and the island of Comino.

Especially on the island of Malta, the stratigraphic sequence is gently tilted towards the NE, resulting in the prevalence of cliffs along the west coast and platforms along the east coast. The Malta Graben is further characterized by numerous fault-line valleys associated with the WSW-ENE-oriented horst-and-graben structures [33–35], which extend offshore (e.g., [28,36]). While the complete stratigraphic sequence can be found in horst domains, the Malta Graben predominantly exhibits the Upper Coralline Limestone (UCL) and Blue Clay (BC). Structural highs bounding the valleys form promontories where the stratigraphic level is slightly higher than in the valleys, most notably along the western edge.

From a geomorphological perspective, the Maltese cliffs can be classified into two groups [37]. The first group comprises vertical cliffs, which are steep vertical or sub-vertical slopes descending towards the sea with a concave-shaped ramp. These cliffs are mostly found in the southwest of the island of Malta and in the west of Gozo, where the LCL outcrops at sea level. The second group consists of screes (locally called rdum), characterized by extensive deposits of slope failures where landslide accumulations cover clayey terrains developed over the BC. This landform primarily occurs in the north of Malta and in the east of Gozo. Deposits consist of chaotic and heterogeneous blocks originating from UCL plateaus, moved mainly by extremely slow-moving landslides such as rock spreads and block slides [38,39].

Using high-resolution bathymetric data, Ref. [40] recognized a rich palaeolandscape in the NE offshore sector of the archipelago that includes palaeoshore platforms and deposits, fluvial valleys, mass movement deposits, terrestrial landforms, and karstic landforms. These authors determined that the Maltese palaeolandscape has been shaped primarily by the same processes that shaped the present-day terrestrial and coastal landscape, which are tectonic activity combined with fluvial, coastal, slope instability, and karst processes.

3. Methods

3.1. Digital Outcrop Models

The Maltese coastal cliffs and promontories are characterized by their difficult accessibility due to various factors such as the high degree of slope, the proximity to the sea, the instability of the slopes, and the presence of a thick accumulation of debris. In addition, the dimensions of the cliffs and the blocks investigated make field observation difficult.

To address these challenges, digital outcrop models of two sites, Sopu and Rdum il-Qammieħ, were created using digital photogrammetry [41] from drone-acquired images. This approach proved to be useful in various promontories across the archipelago (e.g., [14,22,42]). The models allowed a detailed identification and characterization of blocks and fractures that would not have been possible by direct field observations or satellite imagery because of their limited field of observation or limited spatial resolution. In addition, the three-dimensional reconstruction of the promontories made it possible to observe sub-vertical sectors not covered by other aerial data (e.g., aerial orthophotographs). These models provided insights into slope processes and geomorphological dynamics, serving as case studies to extrapolate findings to other promontories with the same stratigraphic configuration.

For the photogrammetric survey, a DJI Mavic 3 Enterprise drone was used and equipped with an RTK antenna and a ground-based GNSS station to ensure precise georeferencing. The flight planning was carried out using DJI Pilot software, where DEMs of the

surveyed areas were integrated. This approach enabled the drone to maintain a constant altitude above the ground surface, ensuring a uniform Ground Sampling Distance (GSD) throughout the survey.

The drone was equipped with a high-resolution camera capable of capturing 20-megapixel images, which facilitated the acquisition of detailed and accurate photogrammetric data and, to enhance the 3D reconstruction of the cliffs, the camera captured nadir images, as well as oblique images at a 45° angle both frontally and posteriorly. The flight parameters were optimized to achieve a frontal image overlap of 85% and a lateral overlap of 70%, ensuring robust photogrammetric processing and minimizing the risk of data gaps.

Processing of the photogrammetric data was conducted using Agisoft Metashape software, following a standard workflow involving a series of consecutive phases [14]. Initially, the camera alignment phase ensured the accurate positioning of geolocated images, generating a sparse point cloud. Following this, the second phase involved constructing a dense point cloud based on estimated camera positions, providing a comprehensive representation of its geometry. In the subsequent phase, a mesh that represents the outcrop surface was derived directly from the dense point cloud. The final phase involved applying textures to the mesh, enhancing visual realism by integrating high-resolution texture data derived from the original images onto the 3D model. From the textured 3D mesh, a high-resolution DEM and high-resolution orthomosaic were derived. The dense point cloud, the textured 3D model, the DEM, and the orthomosaic were used to make detailed observations and measurements of the outcrops through the use of Geographic Information Systems (Table 1).

Table 1. Details of the photogrammetric surveys.

Place	Date	Frontal Overlap	Side Overlap	Photos Aligned/Total	Pixel Size DEM	Pixel Size Orthomosaic
Sopu	September 2021	85%	70%	1472/1475	11.1 cm/pixel	2.77 cm/pixel
Rdum il-Qammieħ	May 2024	85%	70%	3365/3397	13.8 cm/pixel	2.82 cm/pixel

3.2. Remote Sensing Analysis

To expand the field of observations, we study five Maltese promontories (Figure 1), including the two where we performed digital outcrop models (Section 3.1): Għajn Ħammien, Qarraba, Bajda Ridge, Rdum il-Qammieħ, and Sopu. The selection of these promontories is based on their stratigraphic configuration, which consists of the GL-BC contact near sea level and the UCL at the top of the promontory generating a plateau, on the edges of which lateral spreading processes occur.

The frontal and lateral sectors of each promontory were defined to establish a methodological framework for slope analysis. The frontal sector was identified as the area corresponding to the rounded sector of the plateau, usually with the densest accumulations of UCL debris on the slope and roughly coinciding with the major axis of the promontory, while the lateral sectors encompassed the remaining area of the promontory flanks, excluding the frontal sector. It is important to note that the physical boundaries between these sectors are not always clear, and geomorphological and sedimentary characteristics gradually vary. In some cases, such as Sopu, Bjda Ridge, and Rdum il-Qammieħ, the center of the frontal sector and the major axis of the promontory coincide, while in Qarraba and Għajn Ħammien, there is a slight deviation to the northwest.

For each promontory, the maximum and minimum slopes in the frontal and lateral sectors were defined by measuring them from the base of the UCL plateau to sea level, using distance and height differences as reference parameters.

Additionally, two geological cross-sections were reconstructed for each promontory. The first section was drawn laterally across the promontory, while the second section extended from the plateau to the coastline in the frontal sector of the promontory. For the realization of these geological sections, we used a 1 m DSM, provided by the Maltese Planning

Authority (https://www.pa.org.mt (accessed on 10 January 2024)), and a geological map, provided by the Continental Shelf Department of Malta (https://continentalshelf.gov.mt (accessed on 10 January 2024)). We distinguished between different geological units and slope deposits.

Using satellite images obtained from Google Earth Pro (https://www.google.com/earth/about/, retrieved during 15 January 2024), we mapped the most representative landslide deposits of each promontory. For this purpose, we also rely on the observations made on the outcrop models of Rdum il-Qammieħand Sopu Promontory, field observations made at each promontory, and the analysis of the 1 m DSMs, on which we also calculated a Terrain Slope map [43] that facilitated the identification of backtilted blocks.

4. Results

4.1. Main Process Involved in the Relief Rdum Il-Qammieh Promontory

The Rdum il-Qammieħpromontory (Figure 2) features prominent vertical cliffs along the coastline and slopes, which are relatively free of large block deposits. Its upper slope consists of scattered outcrops of the BC, transitioning to outcrops of the GL in the lower part.

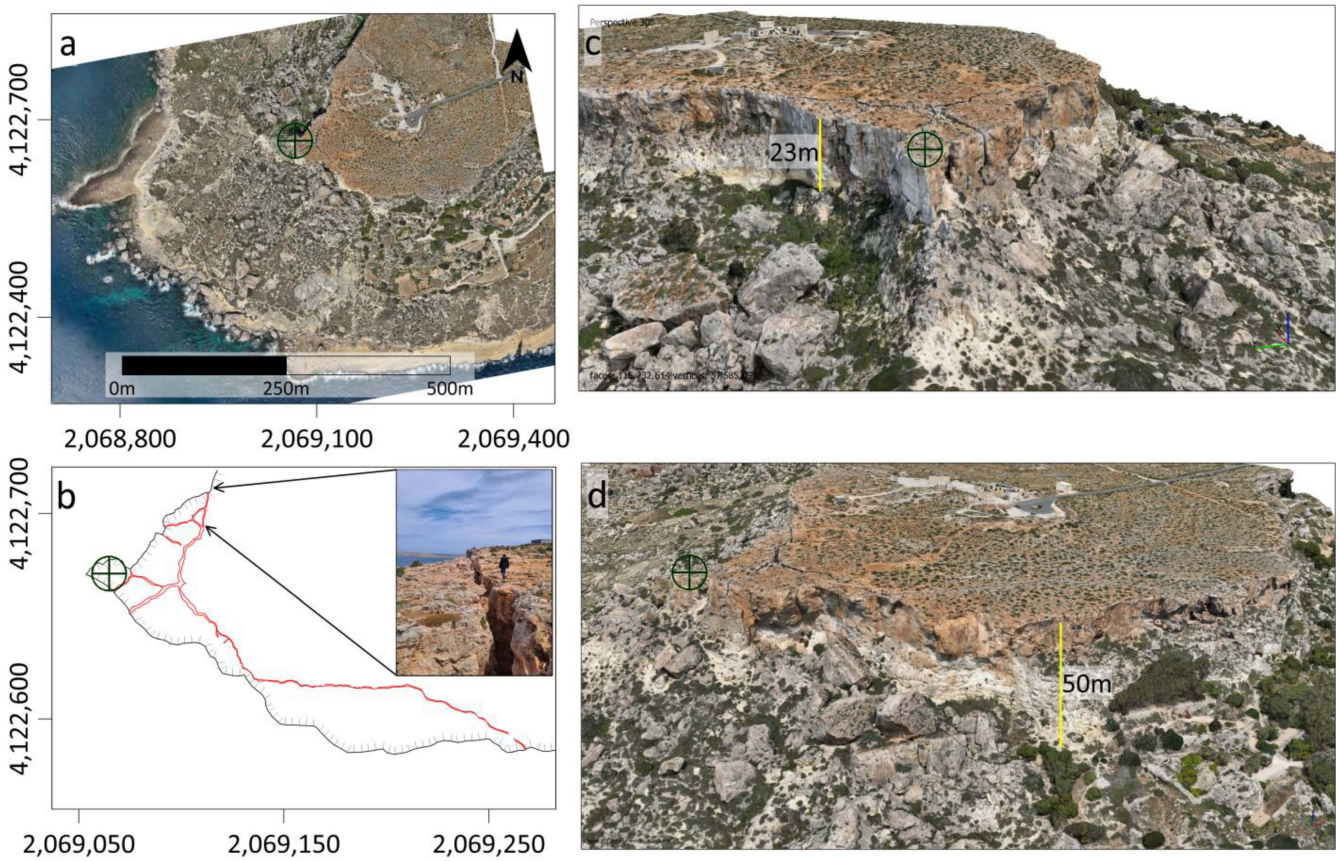

Figure 2. Digital outcrop model of the Rdum il-Qammieħpromontory. (**a**) Orthomosaic of the promontory area. (**b**) Map of the main cracks (in red) and the promontory edge. The scale is the same as in (**a**). (**c**,**d**) Screenshots of the digital outcrop model. The circle with the cross indicates the same location for all the images.

On its SW boundary, fractures are notable on the UCL plateau. A major fracture develops approximately along the perimeter, with a total length of about 250 m, openings up to 2 m, and distances from the plateau edge reaching 35 m. On the E edge of the plateau, several orthogonal fractures with large openings develop and coalesce into the main fracture, creating independent columnar blocks with dimensions around 15 m on each side, though somewhat variable.

The slope of the promontory is covered by blocky debris, broken along the internal stratification planes of the UCL, presumably originating from columnar blocks as described earlier. To a much lesser extent, elongated blocks, individualized by fractures parallel to the edge of the promontory, experience some rotational sliding on the NW boundary of the plateau.

4.2. The Main Process Involved in the Sopu Promontory

The slope stratigraphy of the Sopu promontory is defined by GL at the base, BC throughout the slope, and UCL at the summit; the contact between GL and BC is at sea level [22]. The frontal sector of the promontory is densely covered by blocks, some of which are deep-seated within the sloping terrain and backtilted, being the most prominent features of the sector. The plateau shows inferred cracks based on vegetation alignment, but these have no openings, except for those separating the plateau from the band of subsiding blocks delimiting its NE boundary (Figure 3a–d).

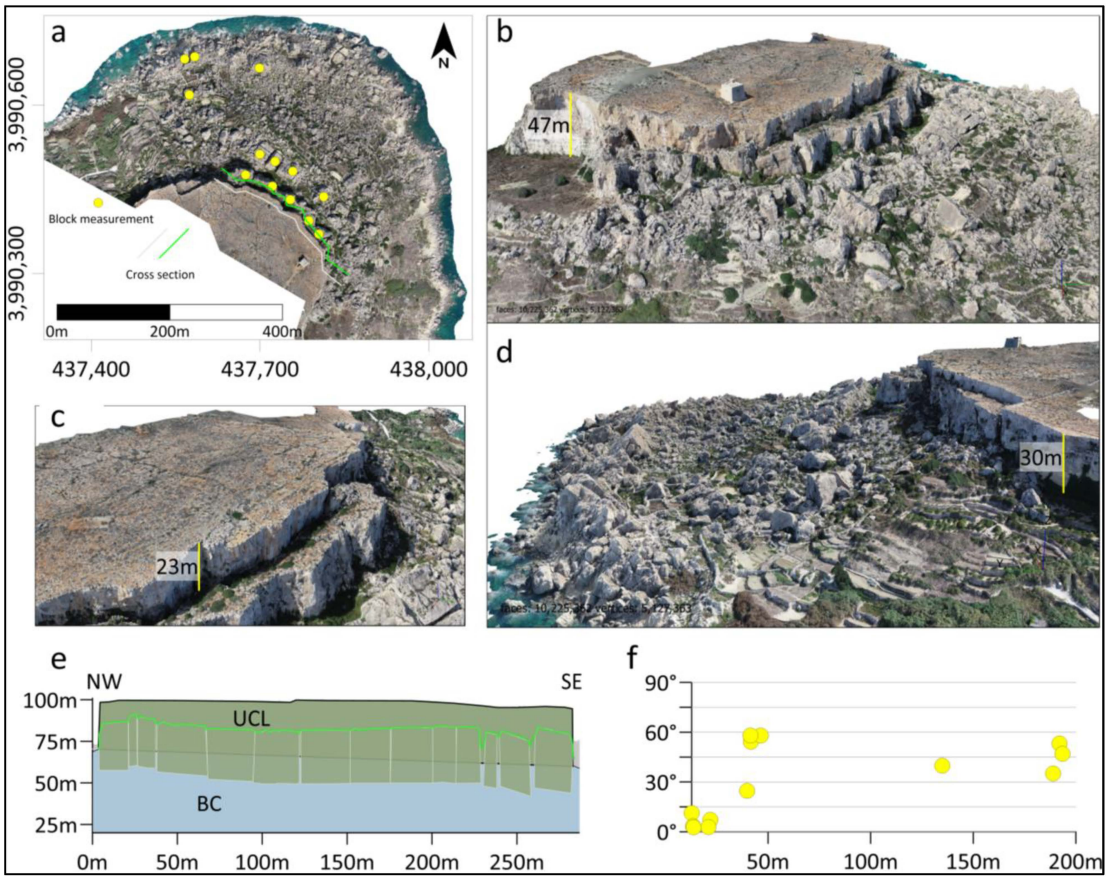

Figure 3. Digital outcrop model of the Sopu promontory. (**a**) Orthomosaic of the promontory area. Green and grey lines represent the cross-section position showed in (**e**). (**b**–**d**) Screenshots of the digital model. (**e**) Cross-section of the plateau and protected sunk blocks (position of the section in (**a**)). (**f**) Chart showing the angle of the tilted blocks as a function of the plateau distance (identified blocks shown in (**a**)).

The relationship between the angle of inclination of the blocks and their distance from the plateau has been analyzed using measurements obtained from the analysis of the orthomosaic, the DSM, and the digital model generated by the same photogrammetry. We measured the distance from the center of 13 backtilted blocks to the edge of the plateau and the angle of inclination of the original surface of each block. These measurements were plotted on an x–y diagram, with distances on the horizontal axis and inclination angles on the vertical axis, as shown in Figure 3f.

The results show that blocks immediately adjacent to the plateau have slight inclinations, generally less than 15 degrees. A second group of blocks located about 45 m from the edge of the plateau shows greater inclinations, between 25 and 60°. Other blocks identified at distances greater than 130 m from the plateau show relatively high inclinations, around 45°.

4.3. Promontory Cross-Sections

A total of 12 geological cross-sections were derived, two for each promontory: one traversing them laterally and another from the plateau to the coast on the promontory's frontal sector. The outcropping geological formations were differentiated as well as the debris covering the slope. In the most emblematic cases, we reconstructed big blocks that are found backtilted. The results are summarized in Figure 4 and Table 2.

Table 2. Details of the promontories obtained from the DSM analysis.

Promontory	Frontal Slope	Lateral Slope	UCL Thickness	BC Thickness	UCL/BC Ratio
Għajn Ħammien	13–28°	16–24°	10–20 m	75 m	0.13–0.26
Qarraba	13–19°	21–41°	15 m	35 m	0.42
Bajda Ridge	10–14°	16–23°	30–45 m	40 m	0.75–1.12
Rdum il-Qammieħ	16–19°	13–16°	30–40 m	45 m	0.66–0.88
Sopu	11–16°	13–18°	25–50 m	50 m	0.5–1

The Għajn Ħammien promontory (Figure 4a) presents significant structural complexities due to the presence of two synthetic normal faults with a NW-SE strike and inclination towards the NE. Frontal slope angles vary between 13 and 28°, being minimal at the base where a large deposit of megaclasts is found. On the sides, slopes range between 16 and 24°.

In section A-A', the slope is concave and gentle due to extension caused by the normal faults. In the middle of the section (x = 180 m), a large block of UCL with backtilting is recognized. Downslope, large clast deposits accumulate, some with characteristics of backtilting, although not easily recognizable. Assuming a sub-horizontal contact for GL and BC formations, the SW fault shows a displacement of approximately 25 m. UCL thickness varies between 10 and 20 m.

Section B-B' shows a notable absence of clast accumulations. The NE slope is gentler compared to the SW due to the influence of the normal faults. The UCL, which crowns the section, presents notable variations in thickness, ranging from 10 to 20 m from SW to NE. The thickness of the BC is greater than in the other promontories, reaching approximately 75 m. The UCL/BC ratio is the lowest among the analyzed promontories, with values ranging from 0.13 to 0.26.

The Qarraba promontory (Figure 4b) forms a small headland and is the smallest and lowest of the studied promontories. It presents frontal slopes between 13 and 19° and lateral slopes between 21 and 41°, developed entirely on the BC. Section A-A' shows a gentle frontal slope, with greater roughness due to UCL megaclasts. Some of these mega blocks, especially near the plateau, are notably backtilted. In this section, a big block is observed, sunk about 5 m from the cliff edge, with no apparent inclination, while other blocks further away show backtilting of 25 to 60° at distances of 30 m and 50 m from the cliff edge, respectively. Section B-B' shows smoother slopes without large megaclast deposits. The southern slope is steep and presents a clean surface where the BC outcrops, while the northern slope is more extensive, less steep, and contains some big block deposits. The UCL has a thickness of approximately 15 m, while the BC outcrops with a thickness of about 35 m, considering the nearest GL outcrop. Considering this partial thickness, the UCL/BC ratio is 0.42.

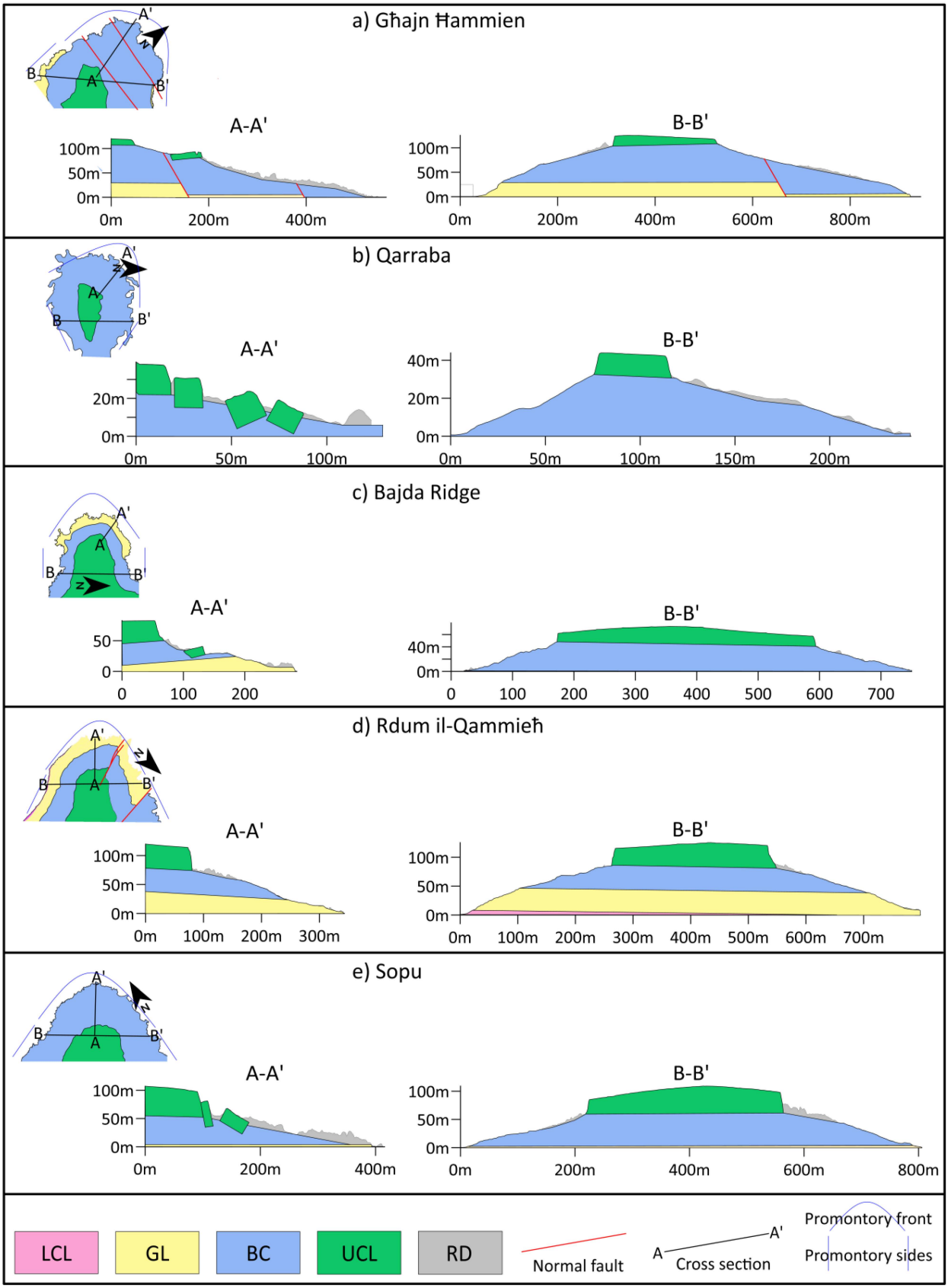

Figure 4. Geological cross-sections of the studied promontories. (**a**) Għajn Ħammien; (**b**) Qarraba; (**c**) Bajada Ridge; (**d**) Rdum il-Qammieħ; and (**e**) Sopu. LCL: Lower Coraline Limestone Fm.; GL: Globigerina Fm.; BC: Blue Clay Formation; UCL: Upper Coraline Formation; and RD: recent deposits.

The Bajada Ridge promontory (Figure 4c) is composed of UCL outcrops on the plateau, BC on the slopes, and at the frontal area, near sea level, outcrops of GL. Frontal slopes vary between 10 and 14°, and along the BC outcrop some backtilted blocks are observed, such as the one represented in section A-A'. The lateral slopes of the promontory are steeper, ranging between 16 and 23°. Along the B-B' section, the UCL thickness varies considerably between 20 and 50 m, with maximum thickness towards the center of the plateau. The BC has thicknesses around 45 m, and the UCL/BC ratio ranges from 0.44 to 1.1.

The Rdum il-Qammieħ(Figure 4d) promontory presents a stratigraphic succession composed of UCL on the plateau and BC and GL on the slope. It is affected by NW-SE striking normal faults, causing certain displacement, especially in the northern sector. In the southern sector, near sea level, outcrops of LCL are recorded. Frontal slopes are steeper, ranging between 16 and 19°, than lateral slopes, between 13° and 16°. In section A-A', block deposits are concentrated near the cliff edge, consisting mainly of fallen blocks without backtilted blocks. Section B-B' is symmetrical, with clastic deposits only on the northern slope, near the cliff edge. UCL thicknesses range between 30 and 40 m, while BC thicknesses are around 45 m, with a UCL/BC ratio of 0.66 to 0.88.

The Sopu promontory (Figure 4e) presents a stratigraphic setting similar to that of Bajda Ridge, with UCL on the plateau, BC on the slope, and GL outcropping near sea level. The frontal slope is covered by large blocks of UCL, producing a highly rough terrain. Frontal slopes range between 11 and 16°, slightly lower than the lateral slopes, which range between 13 and 18°. In the promontory front, in sectors near the plateau edge, blocks are notably sunk and backtilted, as illustrated in section A-A'. Section B-B' shows how clastic deposits of UCL accumulate at the top of the slope, while in the more distal sectors the BC outcrops. The thickness of the UCL varies between 25 and 50 m, and the thickness of the BC is around 50 m, with a UCL/BC ratio between 0.5 and 1.

4.4. Distribution of Main Slope Deposits

To identify the areal sectors where different plateau retreating events predominate, we grouped the clastic deposits into two main categories based on their depositional characteristics, defining an area where these events occur. For this purpose, we utilized field observations and detailed analyses of digital outcrop models, satellite images, and a 1 m resolution LiDAR DSM, to which we applied a slope calculation.

The areas corresponding to deposits of large clasts from fallen and toppled blocks, which characteristically feature broken blocks arranged in a rather chaotic manner due to falling and some downslope transport, were grouped under the name "Block Fall Domain". The areas with deposits of subsiding and backtilted blocks, composed of larger, generally better-preserved blocks whose original surface can be observed tilted towards the plateau, and which may be grouped into belts of blocks that visibly share the same genesis, were grouped under the name "Backtilt Slide Domain". A third group named "Debris Flow Domain" includes debris flow deposits, characterized by a triangular geometry in planar view and smaller blocks with an irregular arrangement. The areas near the current coastline, where block clusters are prone to wave reworking and therefore represent a high degree of uncertainty, were not considered. Areas without blocks or with isolated blocks were also excluded. Additionally, the most significant fractures visible from the satellite images have been mapped.

In Għajn Ħammien (Figure 5a), Block Fall Domains predominate. On the slope of the frontal sector of the promontory, in the N direction, extended fallen blocks are interspersed with some Backtilt Slide Domains. Particularly noteworthy is the one shown in section A-A' of Figure 4a, which likely has a genesis associated with the bordering fault. On the W slope, there is a grouping of fallen blocks that have created a concave edge of the plateau, continuing with a deposit of blocks with a chaotic internal arrangement and a narrow shape that widens downslope, resulting in a semicircular plan view. We categorized this as a debris flow domain.

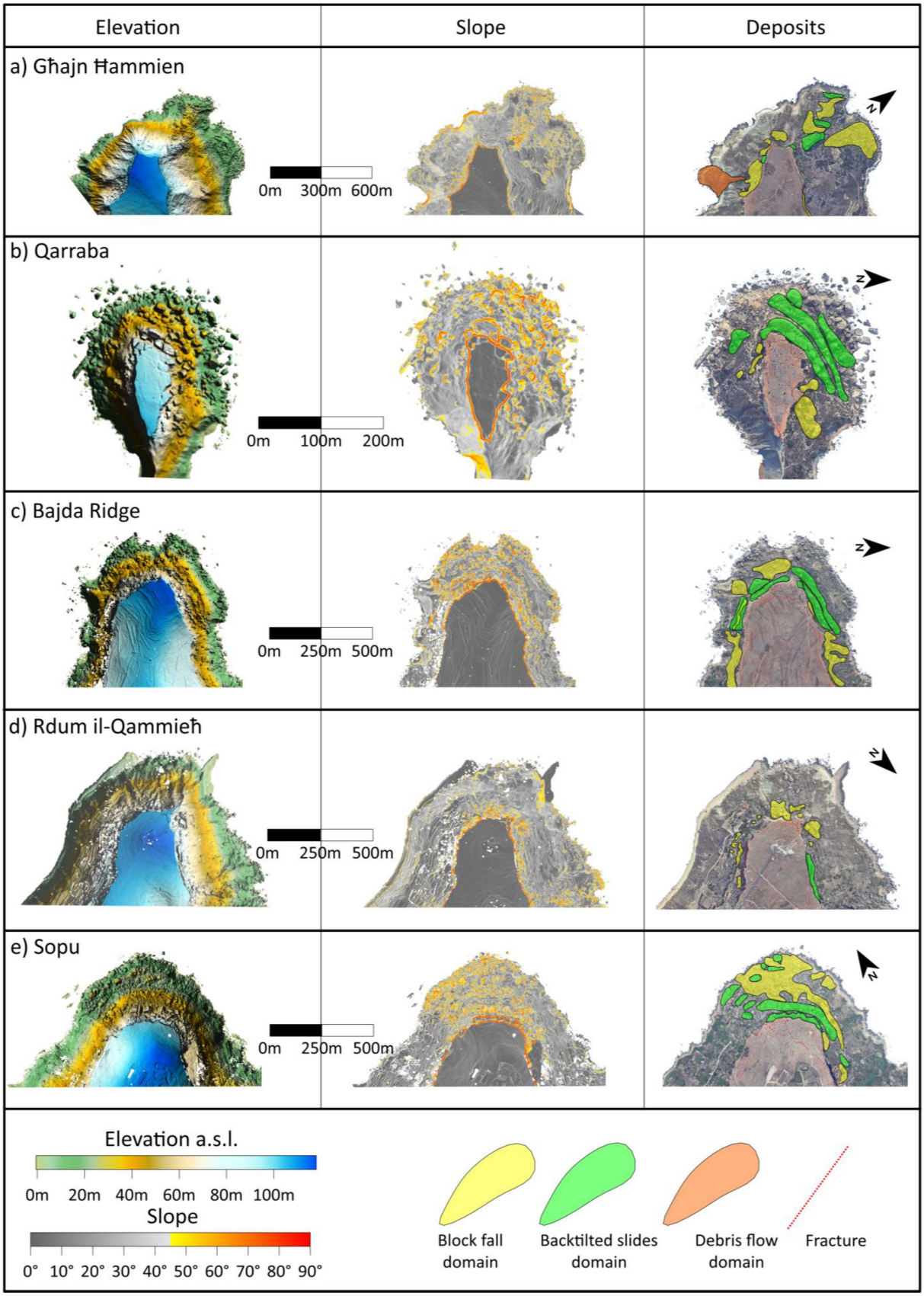

Figure 5. Distribution of different deposit domains at the promontory slopes. (**a**) Għajn Ħammien; (**b**) Qarraba; (**c**) Bajada Ridge; (**d**) Rdum il-Qammieħ; and (**e**) Sopu.

In Qarraba (Figure 5b), subsiding and Backtilt Slide Domains predominate, occurring in at least three belts in the NW sector of the promontory. These blocks, shown in section A-A' (Figure 4b), increase their inclination downslope. Additionally, small areas where Block Fall Domains dominate are found near the plateau, in its lateral sectors.

In Bajda Ridge (Figure 5c), we identified extended areas of subsiding and backtilted blocks in the frontal sector of the cliffs bordering its rounded edge and grouped into up to two belts. Two Block Fall Domains are also recognized on the front of the promontory, as well as on the lateral sides, where no Backtilt Slide Domains are found.

Rdum il-Qammieħ(Figure 5d) does not present large block deposits. Relatively small Block Fall Domains dominate, and only on the NE slope are elongated, parallel-to-the-plateau backtilted blocks recognized.

The Sopu promontory (Figure 5e) is characterized by wide blocky debris on the front of the promontory. In the sector closest to the plateau, two well-differentiated belt of backtilted blocks dominate, contouring the front of the plateau. Other smaller groupings of backtilted blocks are dispersed. Downslope, the deposits become more chaotic and have been interpreted as rockfall deposits.

5. Discussion

5.1. Main Geomorphological Process

The studied promontories are comparable to each other and share a common genesis due to the stratigraphic configuration that promotes fracturing of the UCL plateaus in sectors near the plateau edge, leading to detachment and sliding of blocks downslope.

Cracks are a distinctive feature of the rock-spreading process, observable in the outer sectors of large plateaus on the north coast of Malta. The formation of these gravity-induced joints is due to the opposing geotechnical properties between the stiff UCL formation and the underlying ductile BC Formation. This contrast would generate tensions at the base of the UCL that propagate upward, with lengths that can easily exceed 100 m, partially isolating large rock masses. Once they reach the surface, they are partially filled with clastic material from their walls, acting as wedges. These joints tend to run parallel to the plateau edge, resulting in the recognition of several sets of joints linked to the plateau's geometry, for instance, as documented by [14,19,22]. When the plateau features rectilinear scarps, the individualized blocks tend to be elongated. In non-straight sectors, overlapping joint sets result in the individualization of smaller, equilateral blocks with a tendency towards columnar shapes. Clear evidence of this is in the western corner of the Relief Rdum il-Qammieh plateau, where metric aperture fractures intersect, giving rise to columnar blocks. Once individualized, these blocks tend to topple. Additionally, structurally originated joints and fractures associated with fault zones can also locally contribute to the promontory's evolution, adding to the pattern of gravity-induced cracks.

The subsidence of blocks is another notable feature of these promontories. Once detached, some UCL blocks tend to experience subsidence into the BC. In Sopu, the subsidence reaches percentage values exceeding 50% in the middle sector of the blocks, implying up to 23 m in sectors closer to the cliff. This measurement could indicate the thickness of the BC layer susceptible to more plastic deformation and broadly aligns with the geophysical data presented by [22] in lower sectors of the slope.

Several factors may control subsidence, such as the slope of the hillside, block dimensions and geometry, and the UCL/BC thickness ratio. Higher slopes can destabilize individual blocks and cause them to overturn, while lower slopes, such as those resulting from a higher cliff retreat rate at the promontory's front, favor block stability. Additionally, larger blocks, like those at the rounded promontory front of Sopu, seem to experience subsidence more frequently than smaller blocks, possibly due to their greater mass and the increased gravitational forces acting upon them, which can exacerbate subsidence processes into the BC. Block geometry may also play a crucial role, with blocks having more robust bases being more stable and less prone to falling, thus likely experiencing subsidence and subsequent sliding. The UCL/BC thickness ratio should play a significant

role in UCL block subsidence. The lowest ratio is found in Relief Ghajn Hammien, where large areas of backtilted blocks are absent except for those associated with the fault sector. However, in the eastern sector of the plateau, two relatively small, columnar blocks are recognized as subsided. Qarraba, Bajda, and Sopu promontories show the highest proportion of backtilted blocks. Bajada and Sopu may have ratios equal to or greater than 1, while Qarraba has a calculated UCL/BC ratio of 0.42. Rdum il-Qammieħhas a UCL/BC ratio greater than Qarraba but less than Bajada and Sopu. However, significant accumulations of backtilted blocks are absent, although blocks near the plateau edge, which are currently almost individualized, experience some subsidence.

All observed backtilted blocks also experienced subsidence, a precondition for backward tilting and sliding. Blocks experiencing backward tilting can rotate up to 60° over short distances. In Sopu, blocks rotated up to 60° degrees are found just 50 m from the current plateau. It should be noted that this distance does not necessarily account for the plateau's position at the time of block individualization. Blocks farther from the current plateau position generally do not show inclinations exceeding 60°, suggesting, at least preliminarily, that this angle could be considered a stability measure regarding the rotation process.

The bedding of the geological units plays an important role in determining whether a block evolves by rotating backward and sliding or dipping forward. A slope-facing layer dip would favor the falling of detached blocks, whereas a UCL/BC contact dipping could favor the backward rotation of the blocks. This can be observed in the comparison of Rdum il-Qammieħand Bajda promontories, which have similar stratigraphic configurations. In the former, where the UCL/BC contact tilts towards the promontory front, a few block accumulations indicate that the dominant process is block fall. On the other hand, in Bajada, where the UCL/BC contact tilts towards the island, backtilted blocks are present at the front.

The tectonic configuration is also relevant at the local scale. The clearest case is Għajn Ħammien, where faults control the slope of the promontory's frontal sector and seem to be somewhat related to the presence of backtilted blocks.

5.2. Structural and Sea Level Influences on Maltese Coastal Cliff Development

The coastal geomorphology of the Maltese archipelago has been strongly influenced by sea level oscillation. The regional uplift of the area was completed by Marine Isotope Stage (MIS) 5 in the Late Pleistocene [29], entailing a tectonic stability of the area since the last 125 ky [31,32]. This distinctive setting makes the archipelago a unique example of coastal geomorphology. It seems plausible that the current configuration of the coasts has been mostly impacted by absolute sea level oscillations, rather than tectonic influences in terms of uplift or subsidence documented in several other studies (e.g., [44], among others). The sea level has thus moved along the vertical of the coastline, changing its position several times and interacting differently with the local stratigraphy, especially in terms of erosion and water drainage. The stratigraphy is nevertheless not uniform along the coast of the Maltese islands because of the tectonic setting of the area. In particular, the structural architecture of the archipelago is characterized by a "horst & graben" setting in which it is possible to identify three main geological domains [45]: the Gozo Horst (North of the Gozo Fault), the Malta Graben (between the Gozo Fault and the Great Fault), and the Malta Horst (South of the Great Fault). Older formations in the domains of the Malta and Gozo Horsts and younger outcrops in the Malta Graben area have been exposed due to this geological setting. This explains why GL dominates the coasts of the Malta Graben domain whilst LCL leads the coasts of the horst domains.

The relative sea level curve (RSL) reconstructed by [46] (Figure 6b) demonstrates that the global sea level reached its maximum height (+4.7 m on average above the current s.l.) during the last interglacial (125 ky, MIS-5), and then decreased to the minimum during the Last Glacial Maximum (LGM) (21 ky, MIS-2). The authors of [8] demonstrated that in the Maltese archipelago during the LGM, the sea level was 130 m below the actual level. The

decline in sea level until the LGM was accompanied by further subglacial and interglacial cycles (MIS-4 and MIS-3). Thereafter, the sea level began to rise more or less steadily to its current configuration.

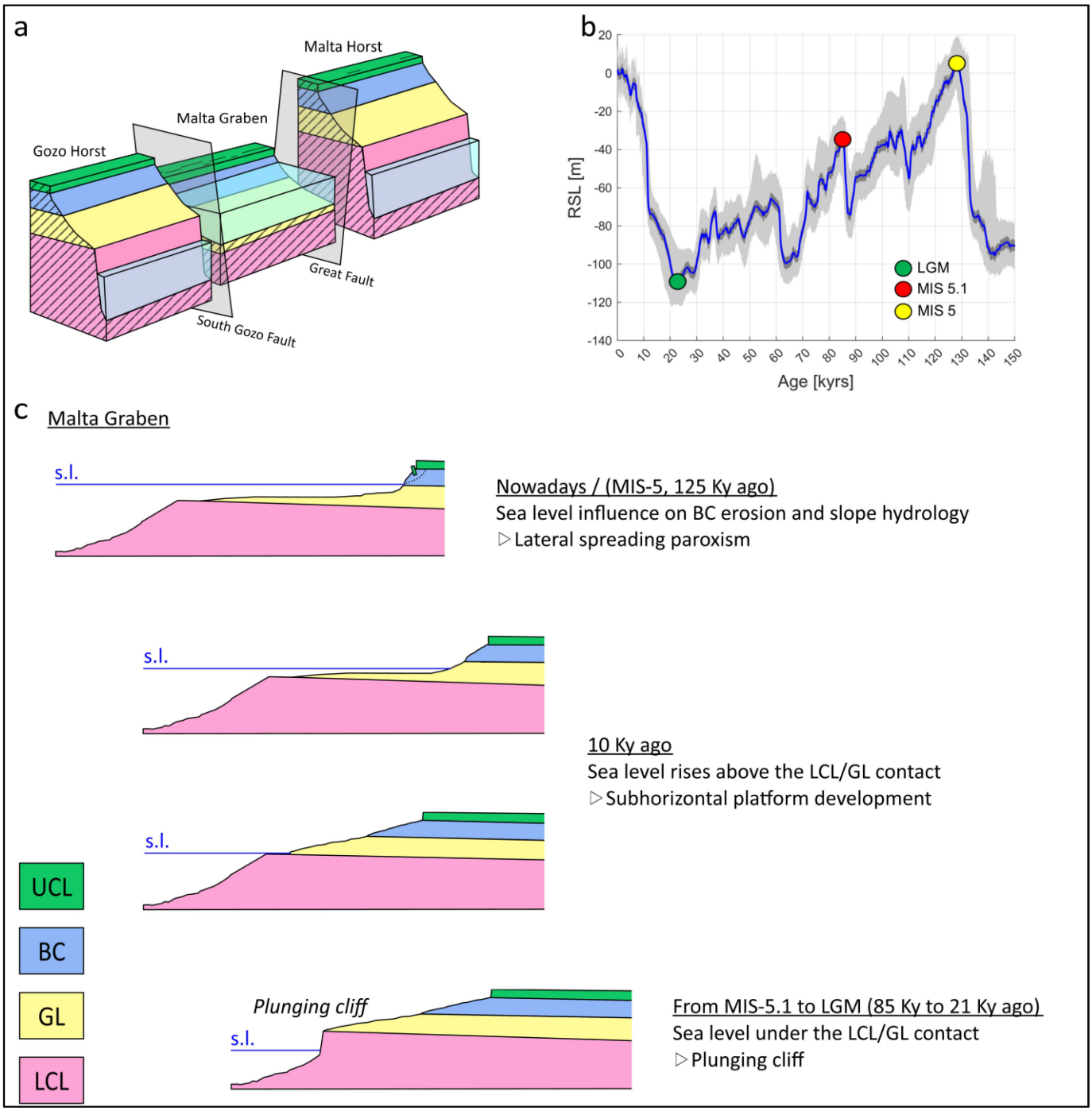

Figure 6. Evolution of the Malta Graben cliffs. (**a**) Sketch showing the structural domains of the Maltese archipelago and their general relation of the cliffs and the sea. (**b**) Relative sea level (RSL) curve (blue) superimposed on the 95% probability interval of the RSL dataset (light gray) (modified from [46]). Last Glacial Maximum (LGM) and Marine Isotope Stages (MIS) 5 and 5.1 are indicated with colored circles. (**c**) Evolution of the Malta Graben cliffs coast over the last 125 ky.

Considering the aforementioned sea level oscillations, it is plausible to assume that during the last 125 ky, the sea level has only interacted with the LCL formation in the

Gozo and Malta Horsts. Sea level excursions from the MIS-5 would not have been able to elevate above the current LCL-GL contact, which averages over 20 m.a.s.l. The coasts in these domains are therefore characterized by a plunging cliff morphology (sensu [1]) with a sub-vertical cliff face (Figure 6a). The lateral spreading processes can be observed along the southwest of Malta and in Gozo, although they do not interact with the sea and are less frequent and less prominent than those in the Malta Graben.

The coasts in the Malta Graben domain are nowadays characterized by a sea level standing close to the GL-BC contact (Figure 6a). Such a geomorphological feature indicates that the sea level interacted not only with the LCL (as for the coast located in the horst domains) but also with the other formations. During glacial periods such as the LGM, the sea level was in contact with the LCL and likely contributed to the formation of plunging cliffs. Similarly to the current setting in the horst domains, lateral spreading processes might have been less dynamic [8]. This setting would have persisted until the sea level approached the LCL-GL or the GL-BC contact during the interglacial stages. The lower resistance to mechanical sea wave erosion of the GL likely played a role in shaping rocky coasts over a previously sculpted landscape, characterized by a sub-horizontal shore platform that ends in a pronounced scarp in the LCL. Eventually, as the sea level approached the GL-BC contact, the erosion surface gently descended from the base of the sea cliff below sea level, without a noticeable topographic break. Sea level standing on the BC formation might have influenced its rheology by contributing to the development of a piezometric level within the formation. The lateral spreading phenomenon may have been facilitated by the partial saturation of the clayey unit, which led to the plasticization of the BC (Figure 6c).

5.3. A Conceptual Model for the Promontory Evolution at the Malta Graben

In this section, a simplified conceptual evolutionary model is presented to explain the morphological evolution of the promontories within the Malta Graben (Figure 7). This model outlines a sequence of stages, detailing the progressive changes in the landscape driven by geodynamic, climatic, and geomorphological processes.

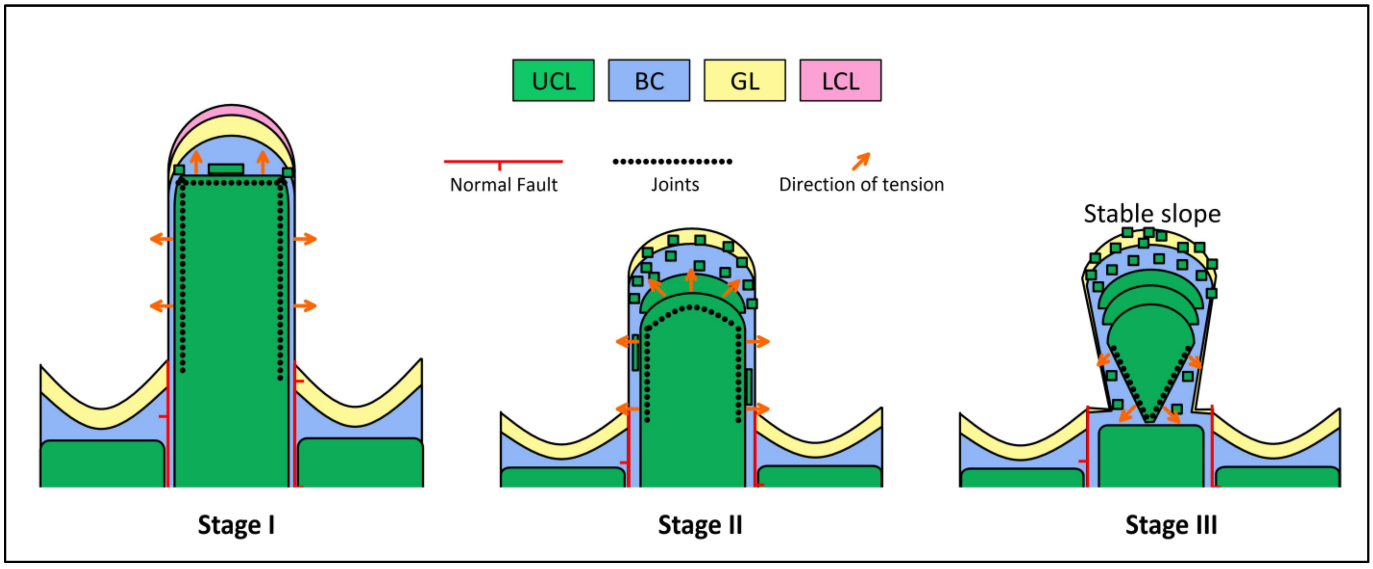

Figure 7. Evolutionary model of a theoretical promontory at the Malta Graben: stage I represents the proto-promontory condition; stage II represents the most intense demolition of the sea cliff; and stage III represents the isolation of a peninsula.

Stage I: Proto-Promontory

The horst and graben structural configuration within the Malta Graben resulted in the structural lows, which coincided with valleys becoming flooded and exposed to wave action as sea levels rose, leading to the formation of bays where beach deposits likely

predominated. In contrast, in the structural highs, which coincided with topographic elevations, promontories began to form, and gravitational slope processes occurred. In this initial stage, the UCL plateaus would present sharp and poorly smoothed edges.

The role of predisposing factors is particularly accentuated, being closely connected to the geological and stratigraphic structure of the area. Elements such as stratification, the relative thickness of formation units, and the geometry of the relief were decisive concerning the mechanisms and speed of the initial gravity-induced slope instabilities.

In the straight sectors of the promontory, joints parallel to the cliff lead to the individualization of elongated blocks. These blocks, being tall and elongated, are inherently unstable and tend to fall once separated from the cliff. Some of these blocks may split due to internal stratigraphic discontinuities acting as planes of weakness, resulting in rock falls. At the corners of the promontory plateau, gravity-induced joint sets intersect, forming a grid pattern that results in relatively small columnar blocks. Due to this process, the detachment, toppling, and falling of blocks are more frequent at the corners due to the intersection of joints, accelerating the retreat of the cliffs in these sectors of the plateau front.

Stage II: Demolition of the cliff

As the sea level approached the LCL/BC contact, the plasticity of the BC increased, promoting the accelerated retreat of the UCL promontory plateaus. An intense demolition phase of the cliffs starts and, as a consequence, the residual platforms facilitate the accumulation of block deposits from the UCL plateaus.

In this phase, the ongoing deformation processes are modified in their evolution (in intensity and rate) by weather–climatic factors and their changes over medium to long periods. The softening of geological units with more ductile behavior is influenced by the water content and their position relative to sea level, which determines their potential submersion. Meanwhile, the fractured walls of the stiff cliffs are exposed to weathering and thermoclastic processes related to diurnal and seasonal temperature cycles.

At the edges of the promontory, the intersection of the joint sets promotes the isolation and falling of blocks, accelerating the retreat of the cliffs in those areas and resulting in characteristic rounded edges. When the plateau has a convex or rounded shape, tensions are distributed outward from the edge, generating a radial pattern. These radial tensions induce fractures that propagate farther from the cliff, allowing the isolation of larger blocks. In contrast, in the straight lateral sectors of the promontory cliff, the fractures remain closer to the cliff, resulting in thinner and elongated blocks.

The large blocks at the promontory front undergo a continuous process of subsidence, tilting backwards, and sliding downhill. This phenomenon can be repeated multiple times at the same front, forming block deposits in semilunar belts. For instance, at sites such as Sopu and Relief Rdum il-Qammieh, at least two landslide accumulations have been recognized, while at Qarraba up to three different accumulations have been identified. Ref. [8] concluded from cosmogenic dating evidence that the development of these landslides likely involved large-scale rupture events, followed by the break-up of the larger displaced blocks by slumps and landslides, generating the numerous dislodged blocks visible today.

If the rate of material accumulation from the blocks of the UCL plateau exceeds the rate at which this material is removed by wave action, it leads to the accumulation of large blocks at the promontory slope, forming a "balance slope" of blocky talus. Nowadays, these blocks can act as a protective barrier against wave action, functioning as a natural breakwater. In places like Sopu, where the front is completely covered by large-sized blocks, fractures on the plateau are not observed to be open, suggesting structural stability. In contrast, in areas like Relief Rdum il-Qammieh, the slopes are steeper and not covered with blocks, presenting edges with gravity-induced joints with openings of up to several meters, indicating a more active dynamic of cliff retreat processes.

On the sides of the promontory, block detachment and the formation of straight cracks continue steadily throughout this stage. The isolation of blocks and their falling remain relatively slow, as the fractures do not intersect. The material generation rate tends to

be lower than the material removal rate, and clastic material does not accumulate on the promontory sides.

Stage III: Isolation of peninsulas

Once the promontory front has stabilized, a potential development is the formation of a peninsula. The cliff retreat processes at the UCL plateau are concentrated on the sides of the promontory, away from the stabilized front, creating a retreat gradient due to the contrast between the stable front and the unstable sides. This can eventually lead to the elimination of the plateau behind the promontory front.

This phenomenon is currently observed in Qarraba, where GNSS monitoring shows higher displacement rates on the sides of the plateau than on the plateau front [47]. The residual state of instability, where the promontories have evolved into isolated reliefs that are strongly altered and disintegrated from the previous evolutionary phases, makes them particularly vulnerable to triggering actions, such as impulsive and highly transient episodes related to earthquakes, intense rainfall, and anthropic activities.

6. Conclusions

This study explores the geomorphological processes shaping the cliffs of the Maltese archipelago, with a particular focus on the evolution of promontories within the Malta Graben. Through remote sensing techniques, we identified and characterized cliff retreat processes, revealing the complex interactions between geological structures, marine erosion, and sea level fluctuations.

The structural configuration of the Maltese archipelago plays a crucial role in its coastal dynamics and actually represents a predisposing factor for the ongoing geomorphological processes. Over the last 125,000 years, plunging cliffs have dominated the horst domains, where sea levels interacted with the LCL. In contrast, the Malta Graben has experienced more intricate processes, including lateral spreading at the BC/UCL contact during sea level rise, leading to accelerated cliff retreat and contributing to the shaping of sub-horizontal shore platforms.

An evolution model of promontories in the Malta Graben was developed through three stages: proto-promontories, cliff demolition, and isolation. These stages are influenced by a combination of predisposing, preparatory, and triggering factors, which govern the stability and transformation of these coastal features under a changing climate.

These findings offer a comprehensive understanding of the evolution of the Maltese cliffs, emphasizing the role of interconnected geological and geomorphological factors. This research not only contributes to the broader understanding of coastal evolution but also contributes to the scientific understanding needed to inform coastal management strategies, with the potential to help preserve these unique and culturally significant landscapes.

Author Contributions: Conceptualization, L.G. and S.M.; methodology, L.G.; software, L.G. and E.C.; validation, L.G., S.D., S.M. and R.G.; formal analysis, L.G. and F.F.; investigation, L.G. and F.F.; resources, S.D. and S.M.; data curation, L.G. and E.C.; writing (original draft), L.G. and F.F.; writing—all authors; visualization, L.G.; supervision, S.M. and S.D.; project administration, L.G.; funding acquisition, S.D. and S.M. All authors have read and agreed to the published version of the manuscript.

Funding: This research received no external funding.

Data Availability Statement: Data are available upon request.

Acknowledgments: Topobathymetric information from ERDF 156 data (2013), Developing National Environmental Monitoring Infrastructure and Capacity, Planning Authority, was used in this work.

Conflicts of Interest: The authors declare no conflicts of interest.

References

1. Sunamura, T. Rocky Coast Processes: With Special Reference to the Recession of Soft Rock Cliffs. *Proc. Jpn. Acad. Ser. B* **2015**, *91*, 481–500. [CrossRef]
2. Gunzburger, Y.; Merrien-Soukatchoff, V.; Guglielmi, Y. Influence of Daily Surface Temperature Fluctuations on Rock Slope Stability: Case Study of the *Rochers de Valabres* Slope (France). *Int. J. Rock Mech. Min. Sci.* **2005**, *42*, 331–349. [CrossRef]
3. Cruden, D.M.; Varnes, D.J. Landslide Types and Processes, Special Report, Transportation Research Board, National Academy of Sciences. *Spec. Rep. Natl. Res. Counc. Transp. Res. Board* **1996**, *247*, 36–75.
4. Hungr, O.; Leroueil, S.; Picarelli, L. The Varnes Classification of Landslide Types, an Update. *Landslides* **2014**, *11*, 167–194. [CrossRef]
5. Carobene, L.; Cevasco, A. A Large Scale Lateral Spreading, Its Genesis and Quaternary Evolution in the Coastal Sector between Cogoleto and Varazze (Liguria—Italy). *Geomorphology* **2011**, *129*, 398–411. [CrossRef]
6. Colica, E.; Galone, L.; D'Amico, S.; Gauci, A.; Iannucci, R.; Martino, S.; Pistillo, D.; Iregbeyen, P.; Valentino, G. Evaluating Characteristics of an Active Coastal Spreading Area Combining Geophysical Data with Satellite, Aerial, and Unmanned Aerial Vehicles Images. *Remote Sens.* **2023**, *15*, 1465. [CrossRef]
7. Mateos, R.M.; Ezquerro, P.; Azañón, J.M.; Gelabert, B.; Herrera, G.; Fernández-Merodo, J.A.; Spizzichino, D.; Sarro, R.; García-Moreno, I.; Béjar-Pizarro, M. Coastal Lateral Spreading in the World Heritage Site of the Tramuntana Range (Majorca, Spain). The Use of PSInSAR Monitoring to Identify Vulnerability. *Landslides* **2018**, *15*, 797–809. [CrossRef]
8. Soldati, M.; Barrows, T.T.; Prampolini, M.; Fifield, K.L. Cosmogenic Exposure Dating Constraints for Coastal Landslide Evolution on the Island of Malta (Mediterranean Sea). *J. Coast. Conserv.* **2018**, *22*, 831–844. [CrossRef]
9. Tomás, R.; Abellán, A.; Cano, M.; Riquelme, A.; Tenza-Abril, A.J.; Baeza-Brotons, F.; Saval, J.M.; Jaboyedoff, M. A Multidisciplinary Approach for the Investigation of a Rock Spreading on an Urban Slope. *Landslides* **2018**, *15*, 199–217. [CrossRef]
10. Furlani, S.; Antonioli, F.; Colica, E.; D'Amico, S.; Devoto, S.; Grego, P.; Gambin, T. Sea Caves and Other Landforms of the Coastal Scenery on Gozo Island (Malta): Inventory and New Data on Their Formation. *Geosciences* **2023**, *13*, 164. [CrossRef]
11. Leucci, G.; Persico, R.; De Giorgi, L.; Lazzari, M.; Colica, E.; Martino, S.; Iannucci, R.; Galone, L.; D'Amico, S. Stability Assessment and Geomorphological Evolution of Sea Natural Arches by Geophysical Measurement: The Case Study of Wied Il-Mielah Window (Gozo, Malta). *Sustainability* **2021**, *13*, 12538. [CrossRef]
12. Sammut, S.; Gauci, R.; Drago, A.; Gauci, A.; Azzopardi, J. Pocket Beach Sediment: A Field Investigation of the Geodynamic Processes of Coarse-Clastic Beaches on the Maltese Islands (Central Mediterranean). *Mar. Geol.* **2017**, *387*, 58–73. [CrossRef]
13. Devoto, S.; Hastewell, L.J.; Prampolini, M.; Furlani, S. Dataset of Gravity-Induced Landforms and Sinkholes of the Northeast Coast of Malta (Central Mediterranean Sea). *Data* **2021**, *6*, 81. [CrossRef]
14. Colica, E.; D'Amico, S.; Iannucci, R.; Martino, S.; Gauci, A.; Galone, L.; Galea, P.; Paciello, A. Using Unmanned Aerial Vehicle Photogrammetry for Digital Geological Surveys: Case Study of Selmun Promontory, Northern of Malta. *Environ. Earth Sci.* **2021**, *80*, 551. [CrossRef]
15. Devoto, S.; Forte, E.; Mantovani, M.; Mocnik, A.; Pasuto, A.; Piacentini, D.; Soldati, M. Integrated Monitoring of Lateral Spreading Phenomena along the North-West Coast of the Island of Malta Coastal Instability Rock Spreading GPS SAR Interferometry GPR Malta. In *Landslide Science and Practice*; Springer: Berlin/Heidelberg, Germany, 2013; pp. 235–242.
16. Galea, P.; D'Amico, S.; Farrugia, D. Dynamic Characteristics of an Active Coastal Spreading Area Using Ambient Noise Measurements—Anchor Bay, Malta. *Geophys. J. Int.* **2014**, *199*, 1166–1175. [CrossRef]
17. Galone, L.; D'Amico, S.; Colica, E.; Iregbeyen, P.; Galea, P.; Rivero, L.; Villani, F. Assessing Shallow Soft Deposits through Near-Surface Geophysics and UAV-SfM: Application in Pocket Beaches Environments. *Remote Sens.* **2024**, *16*, 40. [CrossRef]
18. Iannucci, R.; Martino, S.; Paciello, A.; D'Amico, S.; Galea, P. Engineering Geological Zonation of a Complex Landslide System through Seismic Ambient Noise Measurements at the Selmun Promontory (Malta). *Geophys. J. Int.* **2018**, *213*, 1146–1161. [CrossRef]
19. Iannucci, R.; Martino, S.; Paciello, A.; D'Amico, S.; Galea, P. Investigation of Cliff Instability at Għajn Ħadid Tower (Selmun Promontory, Malta) by Integrated Passive Seismic Techniques. *J. Seism.* **2020**, *24*, 897–916. [CrossRef]
20. Mantovani, M.; Devoto, S.; Forte, E.; Mocnik, A.; Pasuto, A.; Piacentini, D.; Soldati, M. A Multidisciplinary Approach for Rock Spreading and Block Sliding Investigation in the North-Western Coast of Malta. *Landslides* **2013**, *10*, 611–622. [CrossRef]
21. Panzera, F.; Tortorici, G.; Romagnoli, G.; Marletta, G.; Catalano, S. Empirical Evidence of Orthogonal Relationship between Directional Site Effects and Fracture Azimuths in an Active Fault Zone: The Case of the Mt. Etna Lower Eastern Flank. *Eng. Geol.* **2020**, *279*, 105900. [CrossRef]
22. Pistillo, D.; Colica, E.; D'Amico, S.; Farrugia, D.; Feliziani, F.; Galone, L.; Iannucci, R.; Martino, S. Engineering Geological and Geophysical Investigations to Characterise the Unstable Rock Slope of the Sopu Promontory (Gozo, Malta). *Geosciences* **2024**, *14*, 39. [CrossRef]
23. Dart, C.J.; Bosence, D.W.J.; McClay, K.R. Stratigraphy and Structure of the Maltese Graben System. *J. Geol. Soc.* **1993**, *150*, 1153–1166. [CrossRef]
24. Galea, P. Central Mediterranean Tectonics—A Key Player in the Geomorphology of the Maltese Islands. In *Landscapes and Landforms of the Maltese Islands*; Gauci, R., Schembri, J.A., Eds.; Springer International Publishing: Cham, Switzerland, 2019; pp. 19–30, ISBN 978-3-030-15456-1.

25. Micallef, A.; Camerlenghi, A.; Georgiopoulou, A.; Garcia-Castellanos, D.; Gutscher, M.-A.; Lo Iacono, C.; Huvenne, V.A.I.; Mountjoy, J.J.; Paull, C.K.; Le Bas, T.; et al. Geomorphic Evolution of the Malta Escarpment and Implications for the Messinian Evaporative Drawdown in the Eastern Mediterranean Sea. *Geomorphology* **2019**, *327*, 264–283. [CrossRef]
26. Pedley, H.M.; House, M.R.; Waugh, B. The Geology of Malta and Gozo. *Proc. Geol. Assoc.* **1976**, *87*, 325–341. [CrossRef]
27. Hunt, C.O. Quaternary Deposits in the Maltese Islands: A Microcosm of Environmental Change in Mediterranean Lands. *GeoJournal* **1997**, *41*, 101–109. [CrossRef]
28. Galone, L.; Villani, F.; Colica, E.; Pistillo, D.; Baccheschi, P.; Panzera, F.; Galindo-Zaldívar, J.; D'Amico, S. Integrating Near-Surface Geophysical Methods and Remote Sensing Techniques for Reconstructing Fault-Bounded Valleys (Mellieha Valley, Malta). *Tectonophysics* **2024**, *875*, 230263. [CrossRef]
29. Pedley, M. The Calabrian Stage, Pleistocene Highstand in Malta: A New Marker for Unravelling the Late Neogene and Quaternary History of the Islands. *J. Geol. Soc.* **2011**, *168*, 913–926. [CrossRef]
30. Villani, F.; D'Amico, S.; Panzera, F.; Vassallo, M.; Bozionelos, G.; Farrugia, D.; Galea, P. Shallow high-resolution geophysical investigation along the western segment of the Victoria Lines Fault (island of Malta). *Tectonophysics* **2018**, *724*, 220–233. [CrossRef]
31. Furlani, S.; Antonioli, F.; Biolchi, S.; Gambin, T.; Gauci, R.; Lo Presti, V.; Anzidei, M.; Devoto, S.; Palombo, M.; Sulli, A. Holocene Sea Level Change in Malta. *Quat. Int.* **2013**, *288*, 146–157. [CrossRef]
32. Serpelloni, E.; Vannucci, G.; Pondrelli, S.; Argnani, A.; Casula, G.; Anzidei, M.; Baldi, P.; Gasperini, P. Kinematics of the Western Africa-Eurasia Plate Boundary from Focal Mechanisms and GPS Data. *Geophys. J. Int.* **2007**, *169*, 1180–1200. [CrossRef]
33. Alexander, D. A Review of the Physical Geography of Malta and Its Significance for Tectonic Geomorphology. *Quat. Sci. Rev.* **1988**, *7*, 41–53. [CrossRef]
34. Gauci, R.; Scerri, S. A Synthesis of Different Geomorphological Landscapes on the Maltese Islands. In *Landscapes and Landforms of the Maltese Islands*; Gauci, R., Schembri, J.A., Eds.; Springer International Publishing: Cham, Switzerland, 2019; pp. 49–65, ISBN 978-3-030-15456-1.
35. Pedley, H.M.; House, M.R.; Waugh, B. The Geology of the Pelagian Block: The Maltese Islands. In *The Ocean Basins and Margins*; Nairn, A.E.M., Kanes, W.H., Stehli, F.G., Eds.; Springer: Boston, MA, USA, 1978; pp. 417–433, ISBN 978-1-4684-3039-4.
36. Micallef, A.; Spatola, D.; Caracausi, A.; Italiano, F.; Barreca, G.; D'Amico, S.; Petronio, L.; Coren, F.; Facchin, L.; Blanos, R.; et al. Active Degassing across the Maltese Islands (Mediterranean Sea) and Implications for Its Neotectonics. *Mar. Pet. Geol.* **2019**, *104*, 361–374. [CrossRef]
37. Said, G.; Schembri, J. Malta. In *Encyclopedia of the World's Coastal Landforms*; Springer: Dordrecht, The Netherlands, 2010; Volume 1, pp. 751–759, ISBN 978-1-4020-8638-0.
38. Biolchi, S.; Furlani, S.; Devoto, S.; Gauci, R.; Castaldini, D.; Soldati, M. Geomorphological Identification, Classification and Spatial Distribution of Coastal Landforms of Malta (Mediterranean Sea). *J. Maps* **2014**, *12*, 87–99. [CrossRef]
39. Devoto, S.; Biolchi, S.; Bruschi, V.M.; Furlani, S.; Mantovani, M.; Piacentini, D.; Pasuto, A.; Soldati, M. Geomorphological Map of the NW Coast of the Island of Malta (Mediterranean Sea). *J. Maps* **2012**, *8*, 33–40. [CrossRef]
40. Micallef, A.; Foglini, F.; Le Bas, T.; Angeletti, L.; Maselli, V.; Pasuto, A.; Taviani, M. The Submerged Paleolandscape of the Maltese Islands: Morphology, Evolution and Relation to Quaternary Environmental Change. *Mar. Geol.* **2013**, *335*, 129–147. [CrossRef]
41. Linder, W. *Digital Photogrammetry*; Springer: Berlin/Heidelberg, Germany, 2009; ISBN 978-3-540-92724-2.
42. Devoto, S.; Macovaz, V.; Mantovani, M.; Soldati, M.; Furlani, S. Advantages of Using UAV Digital Photogrammetry in the Study of Slow-Moving Coastal Landslides. *Remote Sens.* **2020**, *12*, 3566. [CrossRef]
43. Moore, I.D.; Gessler, P.E.; Nielsen, G.A.; Peterson, G.A. Soil Attribute Prediction Using Terrain Analysis. *Soil Sci. Soc. Am. J.* **1993**, *57*, 443–452. [CrossRef]
44. Della Seta, M.; Martino, S.; Scarascia Mugnozza, G. Quaternary Sea-Level Change and Slope Instability in Coastal Areas: Insights from the Vasto Landslide (Adriatic Coast, Central Italy). *Geomorphology* **2013**, *201*, 462–478. [CrossRef]
45. Prampolini, M.; Gauci, C.; Micallef, A.S.; Selmi, L.; Vandelli, V.; Soldati, M. Geomorphology of the North-Eastern Coast of Gozo (Malta, Mediterranean Sea). *J. Maps* **2018**, *14*, 402–410. [CrossRef]
46. Grant, K.M.; Rohling, E.J.; Ramsey, C.B.; Cheng, H.; Edwards, R.L.; Florindo, F.; Heslop, D.; Marra, F.; Roberts, A.P.; Tamisiea, M.E.; et al. Sea-Level Variability over Five Glacial Cycles. *Nat. Commun.* **2014**, *5*, 5076. [CrossRef] [PubMed]
47. Mantovani, M.; Bossi, G.; Dykes, A.P.; Pasuto, A.; Soldati, M.; Devoto, S. Coupling Long-Term GNSS Monitoring and Numerical Modelling of Lateral Spreading for Hazard Assessment Purposes. *Eng. Geol.* **2022**, *296*, 106466. [CrossRef]